The Influence of Elastic and Inelastic Scattering on Electron Momentum Spectroscopy data

M. Vos *,C. Bowles, A.S. Kheifets and M. R. Went

Atomic and Molecular Physics Laboratory, Research School of Physical Sciences and Engineering, The Australian National University, Canberra, Australia 0200

Abstract

Electron Momentum Spectroscopy (EMS) measures the spectral function of matter directly, provided that multiple scattering effects are small. Even for the thinnest films this is not the case and one has to correct for multiple scattering effects in order to retrieve the spectral function. Both elastic and inelastic scattering effects affect the measurement. Elastic scattering is expected to increase greatly with increasing atomic number, much more so than inelastic scattering. For this reason EMS was thought to be of limited value for heavy targets. Here we present data for carbon silicon and gold and show that they are affected in different ways by multiple scattering. The gold sample has poor count rate, but in the spectra the multiple scattering effects *appear* rather minor. Carbon and silicon on the other hand has good count rate, but the spectra are strongly affected by multiple scattering. Monte Carlo simulations are used to understand these effects. Rather surprisingly the EMS spectra for heavy elements are of comparable quality as those of lighter elements.

Key words: Electron Momentum Spectroscopy, elastic scattering, inelastic scattering band structure;

1 Introduction

Electron momentum spectroscopy (EMS) is a scattering experiment that is able to determine the electronic structure of matter[1]. In this experiment an incoming electron with keV energy has a binary collision with an electron of the target. Because of the energy transfer in the collision the target electron is ejected and both scattered and ejected electrons are detected in coincidence

* Corresponding Author
Email address: maarten.vos@anu.edu.au (M. Vos).

(for this reason the technique is often referred to as (e,2e) spectroscopy). The difference of the sum of the (measured) energy of the outgoing electrons ($E_{1,2}$) and that of the incoming electron (E_0) is the ionisation energy ε.

$$\varepsilon = E_0 - E_1 - E_2 \tag{1}$$

In the same way the difference of the sum of the momenta of the outgoing electrons ($\mathbf{k}_1 + \mathbf{k}_2$) and the incoming momentum $\mathbf{k}_0$ is the recoil momentum $\mathbf{q}$ of the target.

$$\mathbf{q} = \mathbf{k}_0 - \mathbf{k}_1 - \mathbf{k}_2 \tag{2}$$

The frequency that a coincidence events are observed with a certain $\varepsilon, \mathbf{q}$ combination is proportional to the magnitude of the spectral function $A(\varepsilon, \mathbf{q})$. In a independent particle approximation the measured intensity at $\varepsilon, \mathbf{q}$ is proportional to the probability that a target electron has binding energy ε and momentum $-\mathbf{q}$.

This technique works beautifully for gas-phase targets where the target density is low, and the (e,2e) event is virtually always the only scattering event [1,2]. For condensed matter the probability that additional scattering events occur before and/or after the (e,2e) event is significant, even for the thinnest film. If the incoming electron, or one of the outgoing electrons is deflected by a nucleus (elastic scattering) its momentum changes and the wrong recoil momentum of the (e,2e) event is inferred. By the same token if one of the incoming and or outgoing electrons excites the target electron system (inelastic scattering e.g. plasmon creation) its energy changes and the wrong value for ε is obtained.

As the probability of interaction of the incoming and outgoing electrons decreases with increasing energy one can minimise the probability of multiple scattering by increasing the energy of the incoming and outgoing electrons. Hence our present spectrometer operates at relative high energies ($E_0 = 50$ keV, $E_{1,2} \approx 25$ keV) [3] and the multiple scattering effects are small, at least for the thinnest films and low Z targets. The main quasi-particle structure is well resolved which can be compared to band structure calculations. The information contained in the measurement is richer than just the dispersion. Good agreement between the experimental data and theory is only obtained, if one corrects the experiment for multiple scattering and one uses calculations that go beyond the independent particle approximation [4–6].

In this paper we want to explore these multiple scattering effects, especially the possibility of EMS from heavy targets. We compare the case of a light element and a heavy element. Changing the atomic number Z changes the ratio of elastic and inelastic scattering event, which turns out to have a large influence on the observed spectra. We also explore the relationship between sample thickness, coincidence count rate and spectral shape. The results obtained for a heavy target Au are surprisingly good, in spite of intense elastic scattering. The gold data are compared with band structure calculations.

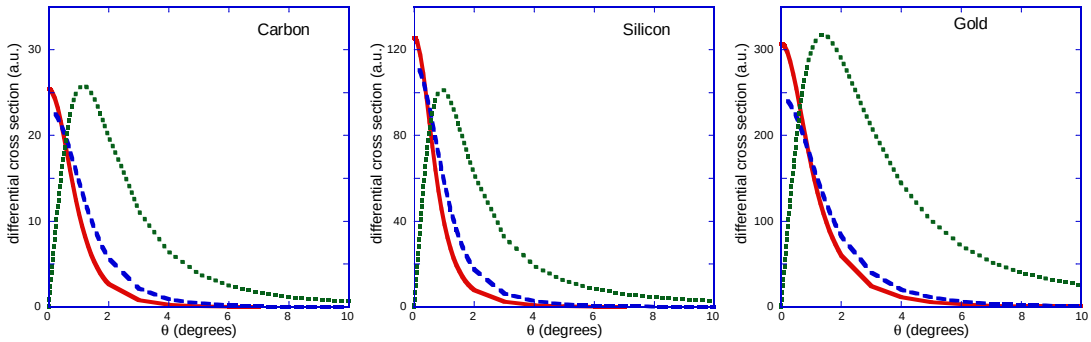

Fig. 1. The calculated differential elastic scattering cross section for 25 keV (dashed line) and 50 keV (solid line)electrons scattering from C (left), Si (central) and Au (right panel.). Note the difference in the vertical scale of the three plots. The dotted line presents the (scaled) probability distribution that a 25 keV electron scatters over an angle Θ integrated over all azimuthal angles

2 Elastic and inelastic scattering cross sections

We now want to discuss briefly the influence of elastic and inelastic scattering. Elastic scattering occurs mainly when the electron is subjected to a strong electric field: ie close to the nucleus. Here there is no large difference between the potential in an isolated atom and an atom in solid. Therefore elastic scattering cross sections used for atoms in solids are usually those obtained from calculations for isolated atoms. In Fig. 1 we plot the differential elastic cross section as calculated using the program PWADIR of Mayol and Salvat [7].

It is immediately clear that the elastic scattering cross section from carbon is about an order of magnitude smaller than that of Au. Moreover the deflection for scattering from Au will generally be larger than that for scattering from carbon. In table 1 the total cross section obtained from this calculation is given, as well as the transport cross section. The larger transport cross section reflects again the fact that scattering from Au involves generally larger angles than scattering from C. The elastic mean free path λ_{el} is inversely proportional to the total cross section and the density of scatterers in the target N: $\lambda_{el} = 1/(\sigma_e N)$.

In contrast to elastic scattering inelastic scattering is a process in the solid, rather than near a nucleus. It depends, among other things, on the valence electron density in the solid. Unfortunately little information is available for the present energy range (25-50 keV). We calculated values using the semi-empirical expression given by Tanuma *et al*[8] for electrons with energy E (in eV) and λ (in Å):

$$\lambda \approx E/[E_p^2 \beta \ln(\gamma E)] \tag{3}$$

with E_p the plasmon energy, β and γ tabulated parameters [8]. This formula was developed for XPS energies (up to 2 keV), and the current extrapolation

Element	E(keV)	σ_{el} (Å^{-2})	$\sigma_{tr.}$(Å^{-2})	λ_{el}(Å)	λ_{in}^{XPS}(Å)	λ_{in}^{EELS}(Å)
C	25	2.5 10^{-2}	1.3 10^{-4}	227	396	310
C	50	1.3 10^{-2}	3.6 10^{-5}	437	729	630
Si	25	8.8 10^{-2}	6.0 10^{-4}	227	356	299
Si	50	4.8 10^{-2}	1.8 10^{-4}	416	654	510
Au	25	4.6 10^{-1}	1.2 10^{-2}	37	170	188
Au	50	3.1 10^{-1}	4.1 10^{-3}	55	310	322

Table 1
A summary of the relevant elastic cross section, transport cross section and elastic and inelastic mean free paths based on an approximate formula developed for XPS [8] and an approximate formula developed for EELS [9]

to 50 keV is pushing the limits, as relativistic corrections are significant at 50 keV.

An alternative approach is to use mean free path values obtained in the literature for electron energy loss spectroscopy (EELS) and extrapolate these to smaller energies. Here a semi-empirical formula was proposed by Malis et al.[9] for λ in nm and E in keV.

$$\lambda \approx \frac{106FE}{E_m \ln(2\delta E/E_m)} \tag{4}$$

with $E_m = 7.4Z^{0.36}$, $\delta = \sqrt{E_p/E}$ and F a relativistic correction factor:

$$F = \frac{1 + (E/1022)}{(1 + (E/511))^2} \tag{5}$$

The similarity between Eq. 3 and Eq. 4 seems to suggest that a unified approach should be possible. Some numeric values are given in table 1. Plitzko and Mayer [10] measured recently for silicon a mean free path of 880 Å at 120 keV whereas the semi-empirical formula gives values near 1000 Å [9].

A different angle to the problem is to consider the ratio of the elastic cross section $\sigma_e l$ to the inelastic cross section σ_{in}. Egerton derived a simple approximate formula: $\sigma_{in}/\sigma_{en} = \lambda_{el}/\lambda_{in} \approx 17/Z$ where we used $\lambda = 1/N\sigma$ with N the number of atoms per unit volume [11]. Thus for C the inelastic cross section is larger than the elastic cross section, for Si both are of the same order and for Au the elastic cross section is considerable larger than the inelastic one. Inspection of the ratios of $\lambda_{el}/\lambda_{in}$ in table 1 show that the values for Au are in reasonable agreement with this formula but for Si and C $\lambda_{el}/\lambda_{in}$ is too small.

In summary there is a some uncertainty in the inelastic cross sections in our energy range. In going from light to heavy elements the elastic mean free paths decrease dramatically, whereas the inelastic mean free paths decreases much more modestly.

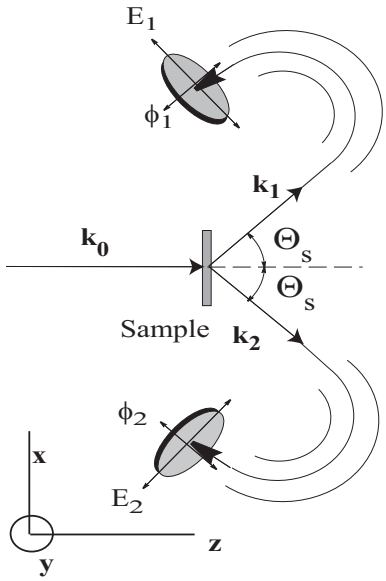

Fig. 2. Schematic representation of the spectrometer

3 Coincidence count rate for extremely thin samples

Our spectrometer, outlined in Fig. 2 has two electron analyzers,each equipped with conical slit lenses [3] and positioned at 44.3°. Incoming electrons have an energy of 50 keV (momentum 62.07 a.u. (we will work in atomic units ($\hbar = m = c = 1$), multiply momentum values by 1.89 to convert a.u. in Å^{-1})), the scattered and ejected electron have an energy near 25 keV (momentum 43.36 a.u.). The analyzers use resistive anodes and, at a mean pass energy of 400 eV, detects electrons over a 70 eV range with a resolution of 0.6 eV. It is instructive to investigate how the count rate in each detector changes as a function of energy (keeping the incoming energy constant at 50 keV). This is shown in figure 3 for an extremely thin carbon film. This count rate shows a broad distribution (on a background) with a maximum near 25 keV. This is a Compton profile of the target electron momentum distribution (and this type of measurement has been studied in an electron microscope [12]). The energy loss of the incoming electron (momentum k_0) after scattering from a target electron with momentum $\mathbf{q}$ is given by:

$$\Delta E = \frac{|\mathbf{K}|^2}{2m} + \frac{\mathbf{K} \cdot q}{m} \tag{6}$$

with m the electron mass and $\mathbf{K} = \mathbf{k}_0 - \mathbf{k}_1$ the momentum transfer, which has a magnitude close to 43.36 a.u. in this experiment. This distribution has a maximum at an energy of 25 keV and here only electrons with $\mathbf{K} \cdot \mathbf{q} = 0$ contribute to the count rate. For a free electron gas with the same electron density as graphite the Fermi sphere radius would be 1.25 a.u. and the base width of the Compton profile is then $2|K|\ k_f = 2.9$ keV, and even this rough model is in good agreement with the experiment. Note that the Compton peak

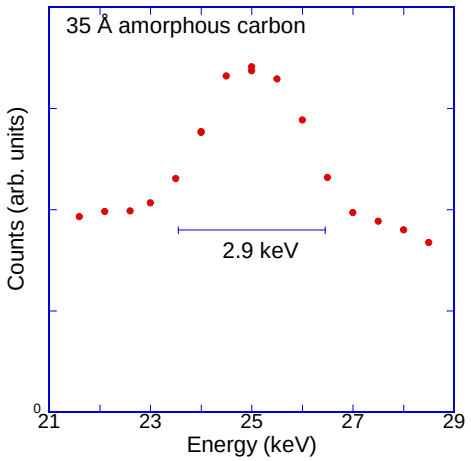

Fig. 3. The Compton profile of a carbon film as measured for 50 keV electrons in an analyser positioned at 44.3°.

is on a rather constant background. The origin of this constant contribution is not known. Under (e,2e) conditions about half the singles counts will be due to Compton scattered electrons.

At 25 keV only electrons within a disk as indicated in Fig. 4 (right panel) will contribute to the count rate. The width of this disk Δk is determined by the range of electrons energies (70 eV) that are detected simultaneously in the detector and is 0.06 a.u. in our case. However due to the finite slit width (0.5 mm,150 mm away from the target) we collect electrons scattered over a (small) range of anglesθ. This deteriorates the momentum resolution to about 0.1 a.u. The total volume of the disk within the Fermi sphere that can cause coincidences is $\pi \Delta k \ k_f^2 = 0.5$ a.u.^{3}. An (e,2e) experiment can be seen as a combination of two Compton experiments. The momentum transfer of the second Compton experiment is perpendicular to that of the first (see 4 (central panel)). Coincidences can only occur for electrons in the overlap of the two Compton disks. It has a volume of $(\Delta k)^2 k_f = 0.0125$ a.u.^{3} i.e. in about 40 times smaller that the volume that can cause a singles count in each detector. In Fig. 5 we show the dependence of the count rate for carbon films on thickness. The thickness are the nominal values quoted by the supplier, but the linear dependence of the singles count rate on sample thickness confirms these values. The coincidence count rate has a maximum near 200-300 Å.

For the thinnest carbon samples there is about one coincidence for every 100 singles counts. This is a surprisingly large number, but in good agreement with our estimate, especially if we realize that this correspond to about 1 coincidence count per 50 Compton-related singles events.

4 EMS of samples of larger thickness

In Fig. 5 we see that only for the thinnest samples the coincidence count rate increases linearly with sample thickness. For larger thicknesses the coincidence

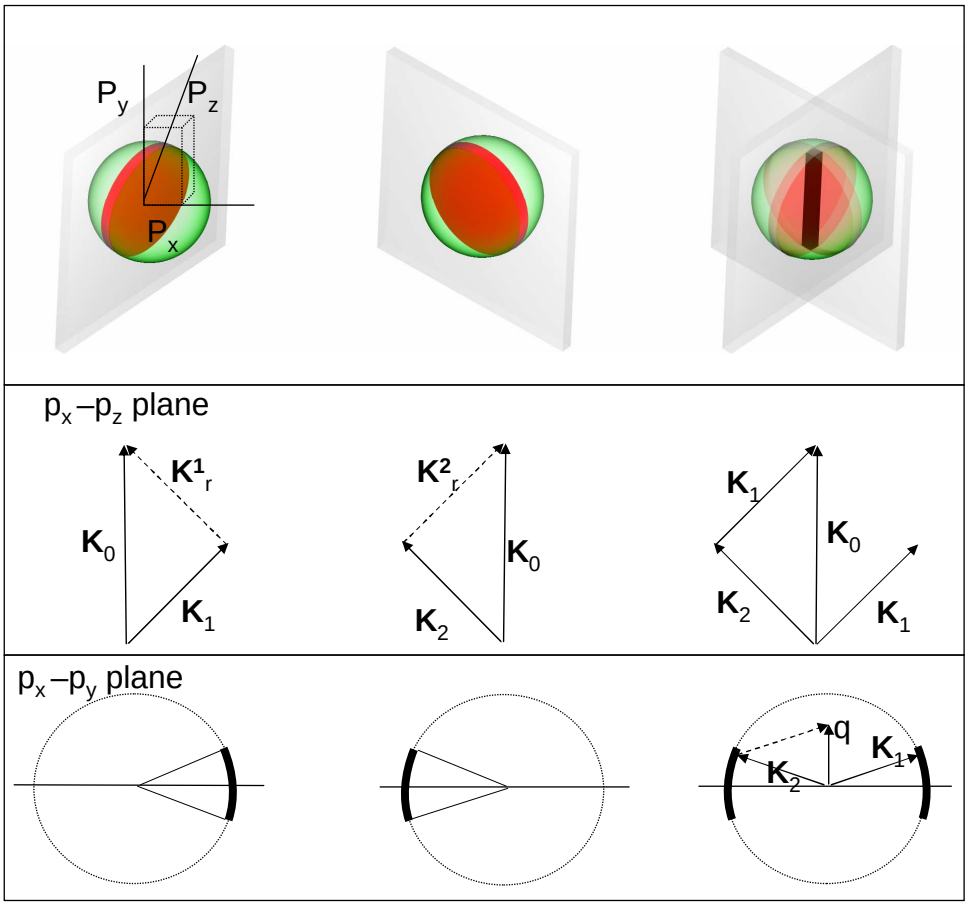

Fig. 4. By detecting electrons with energies close to 25 keV we select target electrons with a momentum component along $K < 0.1$ a.u. (for all electrons within the 80 eV energy window of the analyser (left,top panel). Similar considerations hold for singles detected by analyser 2 (central, top panel). Thus coincidences can only occur for electrons whose only momentum component momentum is along the $P-z$ direction. (i.e. moving along the $z-$axis) is equal to the sum of the p_z- component of the detected electrons (right, top panel). In the central row we show the momenta of the incoming and outgoing electrons of the three experiments, as projected in the p_z-p_x plane. In the third row we show a projection of the experiment in the p_z-p_y plane. As the detector have slit lenses extending along the $y-$direction each detector can measure electrons with a range of ϕ values. The momentum transferred to the target in the (e,2e) event $\mathbf{q}$ is directed along the $\mathbf{p_y}$ axis and has magnitude is proportional to $\phi_1 - \phi_2$.

rate flattens out and subsequently starts to decrease however, the singles rate keeps increasing with thickness. The decrease of the coincidence count rate is a consequence of multiple scattering.

If, for example, the scattered electron loses energy by one or more inelastic scattering events it may end up with an energy that is outside the energy window of the analyzer, and hence these processes lead a reduction of the count rate. The same is true for elastic multiple scattering. The target electrons have a momentum of typically 1 a.u. which is much smaller that the incoming and

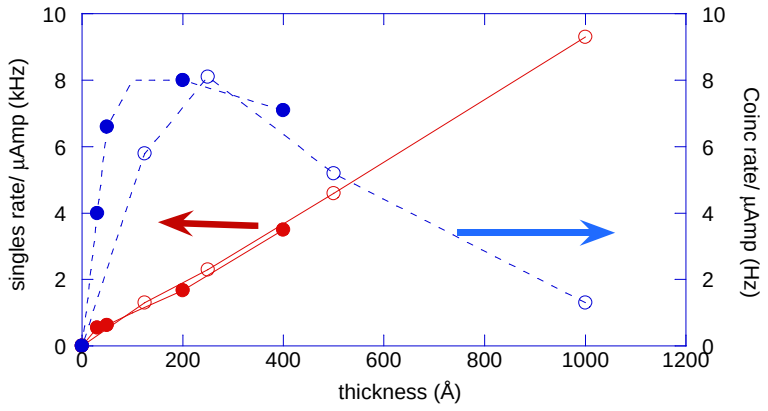

Fig. 5. The singles and coincidence count rate for C (solid circles) and Si (open circles) samples of different thicknesses

outgoing electron momenta. Thus given a certain direction of $\mathbf{k_1}$ there is only a small range of directions of $\mathbf{k_2}$ allowed. The position of detector 2 relative to detector 1 and the incoming beam direction are chosen in such a way that the coincidence count rate is maximised. Changes in $\mathbf{k}_0$, $\mathbf{k_1}$or $\mathbf{k_2}$ due to elastic scattering will reduce the degree of correlation between the direction of both electrons, and hence again reduce the coincidence rate.

If either the energy loss due to inelastic scattering or the deflection due to elastic scattering is large then the event will not contribute to the coincidence count rate. Of more importance are those events that, in spite of small deflections and/or energy losses, still lead to a coincidence event, but for which the subsequently inferred binding energy ε and/or momentum $\mathbf{q}$ as obtained using Eq. 1 and Eq.2 is wrong. This complicates comparison with theory greatly. In the following section we will simulate the effect of multiple scattering for the case of silicon, and see how the ratio of inelastic and elastic mean free path changes qualitatively the outcome of the simulation.

5 Shape of the observed spectra

The optimum thickness for an (e,2e) experiment does not correspond to the thickness with maximum coincidence count rate. Elastic and inelastic multiple scattering do not affect the temporal correlation between the two emerging electrons. For the thicker samples a large fraction of the coincidence events are contaminated by multiple scattering. This fact is dramatically illustrated in Fig. 6 for the case of silicon. Here we present spectra at zero momentum and momentum densities at the valence band maximum. For the thickest samples the measured intensity increases with increasing binding energy, and these spectra contain very little information about the electronic structure. Only for the thinnest sample does the valence band become the most intense feature. The momentum densities at the valence band maximum are less affected by the thickness, increasing thickness mainly causes a reduction in the absolute intensity. These measurements for the $<111>$ direction show clearly the

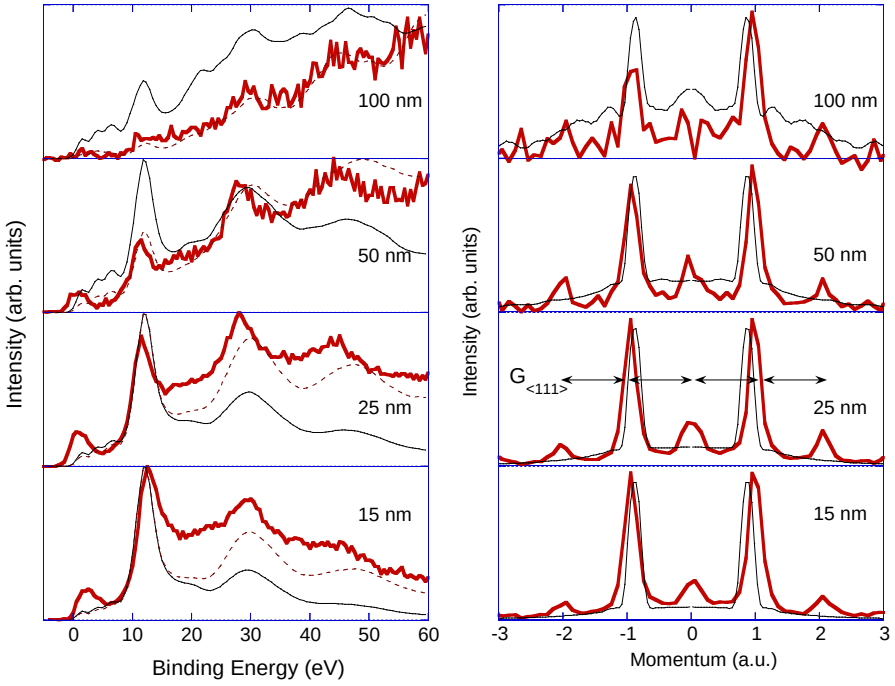

Fig. 6. The dependence of the spectra at zero momentum and the momentum density at the valence band maximum on the thickness of a silicon sample. Simulated spectra (thin line) uses the mean free path as in table 1. The dashed line in the left panel is for a simulation with the elastic mean free reduced by a factor of 2

effect of diffraction: the main peaks at ± 1.0 a.u. is accompanied by minor peaks at 0 a.u. and near 2 a.u., separations corresponding to the smallest reciprocal lattice vector ($|G_{<111>}| = 1.06$ a.u.). For more details see [13,14].

To test our understanding of these processes we performed Monte Carlo simulations, based on a code that has been described previously [15]. The main difference between this earlier version and the current one is that energy distribution of energy loss events is not taken to be a Gaussian distribution centered around the mean plasmon loss energy, but an energy distribution of which the shape was determined in a separate energy loss experiment of the thinnest film available. These results are shown as well in fig. 6. Qualitatively the same tendencies are observed in the experiment and in the simulations. In the experiment there are clear signs of diffraction. These effects are not incorporated in the Monte Carlo simulations, which assume that all elastic collisions of different atoms are incoherent. The main difference is that the effect of thickness seems to be underestimated in the simulations for the energy spectra. A separate simulation was done with the inelastic mean free paths reduced by a factor of 2. This simulation is indicated by a dashed line in fig. 6 and seems to follow the experiment more closely. A similar agreement for the spectra can be obtained by doubling the sample thickness. However this would reduce the agreement in the momentum density profiles.

Part of this problem could be due to intrinsic satellites. These satellites (due to electron-electron correlation, sometimes referred to as 'intrinsic plasmons')

are included in the theory that was used as an input for the Monte Carlo simulations, but the computational scheme used seems to underestimate the intrinsic satellite contribution. A comparison of spectra obtained for silicon with the results of many-body theory is given elsewhere [16,14].

6 EMS of heavy elements

There are two factors that are unfavourable for EMS of heavy targets e.g. gold films. The first factor is an expected reduction in the elastic mean free path. Not only is the elastic mean free path about 5 times smaller in Au compared to Si and C, also the average scattering angle in a deflection is somewhat larger for Au (see fig. 1). The second problem is the presence of many electrons in the sample with large momentum values. E.g the 5d electrons have a momentum of several a.u. Thus their extension in momentum space, as sketched in fig.4 is much larger. This causes a reduction of the ratio of coincidences to singles. Moreover many of core levels (even the shallow ones) will not contribute at all to the coincidence count rate due to energy conservation, but they still contribute to the Compton profile (i.e. singles count rate).

It was thus surprising that an attempted measurement of the electronic structure of Au was successful, even for single crystalline films. Au layers of 1000 Å thickness were grown on an NaCl crystal. The salt substrate was dissolved, the film floated off,transferred to the sample holder wit 0.2mm diameter holes and subsequently sputter-thinned *in situ*. The thickness of the film, as estimated from the EELS data, was 70-90 Å, but is expected to vary around this value, due to the statistical nature of sputtering. Using the Monte Carlo simulation we can estimate which fraction of the (e,2e) event is not accompanied by additional elastic or inelastic multiple scattering events. Only these events contain clear information about the electronic structure of the target. The results of these simulations are presented in table 2. From this table we conclude that for Carbon and silicon we can do (e2e) measurements up to thicknesses of 200 Å (at least 10% of the events are clean), but for Au anything above 50 Å appears prohibitively thick. Even at 50 Å does the simulation overestimate the effects of elastic scattering (see Fig. 7, right panel). A discussion of the obtained spectral density of the Au film will be published in a separate paper [**?**].

Finally we show in fig. 8 the spectra for a Au film over a wider energy range. These spectra were obtained from two measurements over a different binding energy window, with a significant overlap. The valence band features are much stronger than the core levels. This is in strong contrast to XPS spectra that are dominated by the core levels. This is a clear illustration of the difference between the ionization process by photons and by binary collisions. The very localized core levels have very diffuse momentum-space wave functions. Hence the density at any given point in momentum space is small, resulting in low-intensity peaks in the EMS spectra. Orbitals with high angular momentum

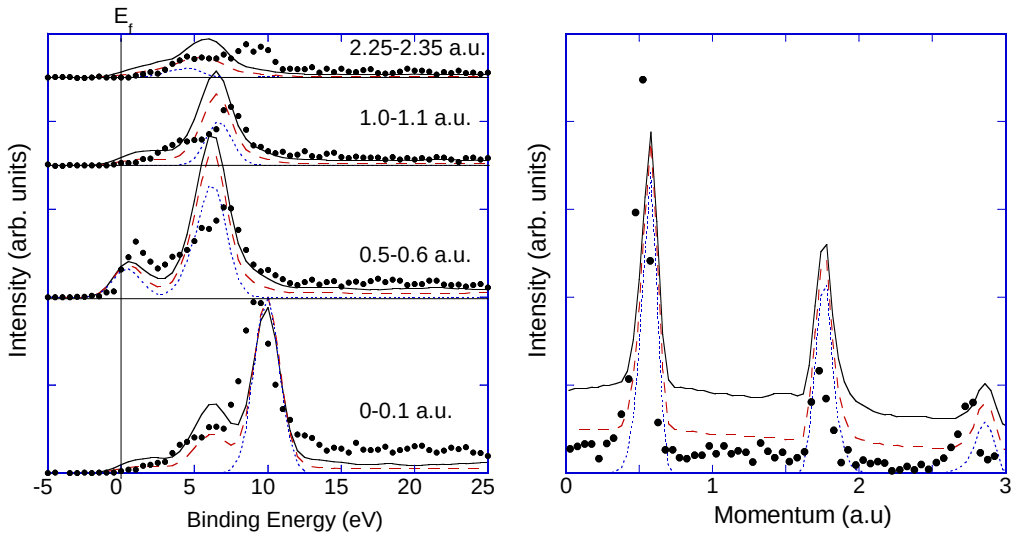

Fig. 7. Spectra at different momentum values as indicated (left panel) as well as the momentum density at E_f (right panel). The short dashed line corresponds with the (LMTO) theory convoluted with experimental energy and momentum broadening. The long dashed (full) line corresponds to the results of Monte Carlo simulations using the LMTO theory and assuming a thickness of 50Å(100 Å)

Element	Thickness (Å)	clean events
C	50	58%
C	100	35%
C	200	14%
Si	50	56%
Si	100	33%
Si	200	13%
Au	50	9.5%
Au	100	1.6%
Au	200	0.1%

Table 2
The percentage of all (e,2e) events that are not contaminated by either elastic or inelastic multiple scattering, as derived from the Monte Carlo simulations

such as the 4f electrons have virtual no density below 1.5 a.u., whereas the 5s electron has maximum density at 0 momentum. The momentum distribution of the 5p electrons is in between that of the 4f and 5s. Note that the 5s binding energy is somewhat larger than that the usual quoted value derived from[17]. This peak is difficult to pinpoint in XPS spectra as it is in the low energy tail from the much more intense 4f peaks.

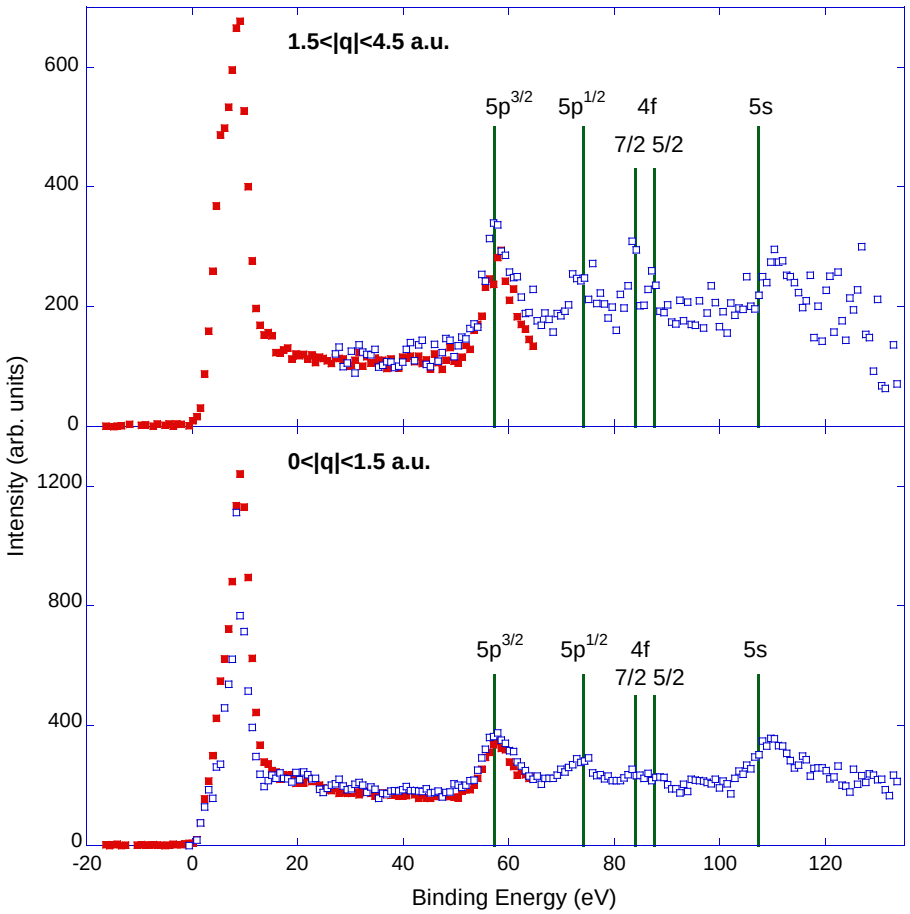

Fig. 8. The measured intensity of a Au film over an extended energy range comprised of two different overlapping scans. In the top panel we show the spectra summed over $1.5 < |q| < 4.5$ and in the lower panel we show the intensity summed over low momenta$< |q| < 1.5$ The 4f signal is weak and only visible in the high momentum region. The energy levels shown are taken from [17].

7 Conclusion and discussion

We have studied the influence of multiple scattering on EMS measurements. Only for the thinnest films of low Z elements, where multiple scattering probability is small, is the count rate proportional to the sample thickness. Here we find a coincidence count rate that is about 1% of the singles count rate. We showed that this ratio can be understood in terms of the phase space of electrons that contribute to singles and the coincidence events. For the low Z elements coincidence count rate drops slowly with increasing film thickness, but more importantly the measured intensity distribution is heavily affected by multiple scattering and the spectrum seems to shift to higher and higher binding energies due to inelastic energy loss processes. For high Z target the count rate is low, even for thin films, but the spectra appear to be much less affected by multiple scattering.

It is possible to simulate the effect of multiple scattering semi-quantitatively.

However generally the effects of elastic multiple scattering are overestimated, whereas the effects of inelastic multiple scattering seems underestimated. The first problem could be attributed to a failure of the incoherent approximation. Especially for small scattering angles (when the momentum transfer k_{el})is such that $|1/k_{el}|$ is of the order of the interatomic separation)one should consider the effects of diffraction. Normally Monte Carlo simulations are used to calculate transport properties, which are not affected severely by small angle deflections. However in the EMS case small deflections cause a significant change in the inferred momentum $\mathbf{q}$ that is associated with the (e,2e) event. Hence a more sophisticated approach could be required.

The fact that inelastic scattering is worse in the experiment compared to the simulation could be a consequence of using the wrong spectral function as input. For silicon the spectral function used incorporated intrinsic plasmons, whereas this was not the case for Au. Judging from the experiments intrinsic plasmons should be less important for Au than for C or Si.

8 acknowledgement

This work was made possible by a grant of the Australian Research Council.

References

[1] E. Weigold, I. E. McCarthy, Electron Momentum Spectroscopy, Kluwer Academic/Plenum, New York, 1999.

[2] I. E. McCarthy, E. Weigold, Electron momentum spectroscopy of atoms and molecules, Rep. Prog. Phys. 54 (1991) 789.

[3] M. Vos, G. P. Cornish, E. Weigold, A high-energy (e,2e) spectrometer for the study of the spectral momentum density of materials, Rev. Sci. Instrum. 71 (2000) 3831–3840.

[4] M. Vos, A. S. Kheifets, E. Weigold, F. Aryasetiawan, Evidence of electron correlation effects in the spectral momentum density of graphite, Phys. Rev. B 63 (2001) 033108.

[5] M. Vos, A. S. Kheifets, V. A. Sashin, E. Weigold, M. Usuda, F. Aryasetiawan, Quantitative measurement of the spectral function of aluminum and lithium by electron momentum spectroscopy, Phys. Rev. B 66 (2002) 155414.

[6] E. Weigold, A. S. Kheifets, V. A. Sashin, M. Vos, Spectral momentum densities in matter determined by electron scattering, Acta Cryst A60 (2004) 104–110.

[7] F. Salvat, R. Mayol, Elastic scattering of electrons and positrons by atoms. schrödinger and dirac partial wave analysis, Comp. Phys. Commun. 74 (1993) 358.

[8] S. Tanuma, C. Powell, D. Penn, Calculations of electron inelastic mena free paths, Surf. Interface Anal. 17 (1991) 911–926.

[9] T. Malis, S. Cheng, R. Egerton, EELS log-ratio technique for specimen thicknes measurement in the tem., J. Electron Micros. Tech. 8 (1988) 193.

[10] J. M. Plitzko, J. Mayer, Quantitative thin film analysis by energy filtering transmission electron microscopy, Ultramicroscopy 78 (1999) 207–219.

[11] R. F. Egerton, Electron energy-loss spectroscopy in the electron microscope, Plenum Press, New York, 1986.

[12] B. G. Williams, T. G. Sparrow, R. F. Egerton, Electron Compton scattering from solids, Proc. R. Soc. A 393 (1984) 409–422.

[13] M. Vos, A. S. Kheifets, V. A. Sashin, E. Weigold, Influence of electron diffraction on measured energy-resolved momentum densities in single-crystalline silicon, J. Phys Chem. Solids 64 (2003) 2507–2515.

[14] C. Bowles, A. Kheifets, V. Sashin, M. Vos, E. Weigold, The direct measurement of spectral momentum densities of silicon with high energy *(e,2e)* spectroscopy, J. Elec. Spec. Relat. Phenom. 141 (2004) 95–104.

[15] M. Vos, M. Bottema, Monte Carlo simulations of (e,2e) experiments in solids, Phys. Rev. B 54 (1996) 5946–5954.

[16] A. S. Kheifets, V. A. Sashin, M. Vos, E. Weigold, F. Aryasetiawan, Spectral properties of quasiparticles in silicon: A test of many-body theory, Phys. Rev. B 68 (2003) 233205.

[17] J. A. Bearden, A. F. Burr, Reevaluation of x-ray atomic energy levels, Rev. Mod. Phys. 39 (1967) 125.